Lowland Technology International 2020; 21 (Issue 4): 255 -267
International Association of Lowland Technology (IALT): ISSN 1344-9656
Special Issue on: Engineering Geology and Geotechniques for Developing Countries

Research Paper

Fault induced problems in hydropower tunnels in Nepal: A case study

B. Chhushyabaga [1], S. Karki [2] and S.S. Khadka [3]

ARTICLE INFORMATION

Article history:

Received: 14 October, 2019
Received in revised form: 11 January, 2020
Accepted: 16 January, 2020
Publish on: 06 March, 2020

Keywords:

Fault,
Hydropower tunnel,
2D Numerical Analysis.

ABSTRACT

This study focuses on the fault induced problems in the hydropower tunnels in Lesser Himalaya Region of Nepal and its stability using Numerical analysis. The presence of fault in the rock mass increases the existing in-situ stress beyond its critical level and strength. Due to which squeezing, swelling in sheared, schistosed, deformed rock mass and spalling, rock bursts in intact, unjointed rock mass are frequently encountered. The existing methods of the stability analysis, estimation of tunnel support using rock mass classifications do not consider the effect of the fault. A detailed study using 2D numerical analysis is carried out using the geological data, rock mass and fault encountered in hydropower tunnel. A comparison is then made between the analysis result of the tunnel with and without the fault to actual tunnel of case study.

1. Introduction

The geology of Nepal is dominated by presence of three principal thrusts: Main Frontal Thrust (MFT), Main Boundary Thrust (MBT), and Main Central Thrust (MCT). The faults in Nepal Himalaya are generally classified as ductile faults and brittle faults. Ductile faults occur at deeper parts with no significant change in mechanical properties of rock mass whereas brittle faults occur close to the earth surface with sheared and loose rock matrix composed of strong to very weak rock blocks (Sunuwar , 2005). The tunnel passing through the faults have different stability problems. They are high deformation, over breaks, running ground and Squeezing (Kang et al.,2018; Zingg and Anagnostou, 2012; Anagnostou and Kalman, 2005). These stability problems cause the failure of the empirically estimated supports. The estimated supports in faulted rock mass in Nepal Himalaya consisting of steel fibre reinforced shotcrete with steel ribs has proved to be inadequate, causing the collapse of the tunnel. Hence, more stiff supports with new steel fibre reinforced shotcrete, steel ribs, H beams have been used as stable support (Shrestha and Panthi, 2014). It is found that the deformation can occur more in the invert level of the tunnel than in the crown or spring line, so steel struts in the invert must be provided (Shrestha and Panthi, 2014).

In 2010, Mezzatesta and Malaguti suggested that flexible supports with high supporting pressures and sufficient deformative resources are required to reduce the rock mass pressure and squeezing. Running ground in cohesionless soil with water and squeezing in low strength cohesive material are the ends of the wide spectrum of problems encountered when tunneling is done in faulted zones. Grouting, drainage and consolidation of the ground ahead of the tunnel face helps to mitigate the above problems (Anagnostou and Kalman, 2005).

In fault fractured rock mass, there is degradation of strength parameters of the rock mass. The degradation index of elastic modulus is 84.06% and internal friction angle is 22.79%. Bolting support and full length anchoring of cement grout with gradual increase in pre-

[1] Graduate Student, Department of Civil Engineering, Kathmandu University, Dhulikhel 45200, NEPAL, bimal.chhushyabaga@ku.edu.np
[2] Graduate Student, Department of Civil Engineering, Kathmandu University, Dhulikhel 45200, NEPAL, Sujan.Karki@ku.edu.np
[3] Assistant Professor, Department of Civil Engineering, Kathmandu University, Dhulikhel 45200, NEPAL, sskhadka@ku.edu.np
Note: Discussion on this paper is open until September 2020

tightening force help in increasing the bearing capacity of the faulted rock mass (Su et al., 2017).

There is serious deformation in the tunnel excavation with ordinary support through the faulted rock mass or dense fracturing, poor integrity, fissure water, high tectonic stress, low strength in surrounding rock mass. Improved support method of long drill pre-grouting pipe roofing, bolts. U-steel support, shotcrete, improved grouting cables, floor cables is an effective method for reinforcing the tunnels in fault zones (Kang et al., 2018).

In 2002, Russo et al. suggested two design methods of tunnel in faulted zone: over excavation and articulated design method. In over-excavation method, tunnel is driven through the fault with enlarged cross section. A double lining is installed and filled by a porous material. When fault rupture occurs, the clearance profile is guaranteed by the gap between the outer linings and inner linings. In articulated design method, the tunnel lining segments are reduced leaving a series of independent sections across the fault and over a certain length beside the fault. This helps to concentrate the movements at the joints linking the segment and accommodate the movement on a certain distance.

The analysis of the tunnel in the faulted rock mass has been done by using 3-D modelling in UDEC, FLAC3D in the context of Nepal Himalaya (Shrestha and Panthi, 2014). However, the analysis is very complex. So analysis of the faulted rock mass incorporating the existing joints have been done in 2-D using RS2 provided by Rocscience. The geotechnical properties required for the modelling have been obtained from laboratory tests, field data and empirical methods. To model the effect of the fault, the in-situ stress (horizontal and vertical) have been calculated using the 2D faulting theory for the reverse faults (Zoback and Zoback, 2002). The measured orientation of the joints sets and their empirically calculated strength parameters have been incorporated in the model to obtain more realistic conditions.

In this study, Kulekhani III Hydropower (27°35'27" N and 85°09'25" E) is located 30 km aerial from the Southwest of the Kathmandu valley in the zone of lower and sub Himalayas in Makwanpur District (**Fig.1**). The general trend of rock is east to west and dips toward north east (**Fig. 2**). The headrace tunnel of diameter 3.5 m, 4.7 km length passes through Marble, sheared schist, Granetiferous schist, Quarzite schist, Schistose Quarzite, Sheared Schists, Quarzite, Phyllite, Sheared Phyllite, Siliceous Dolomite, Slate Phyllite (NEA, 1997). The overburden above the tunnel varies from 120 m to 330 m. Maximum overburden of 330 m is at chainage of 1+450 m and minimum overburden of 120 m is at chainage of 1+430 m.

MBT is located about 600m south of powerhouse site in the tectonic contact between tertiary sedimentary rock and metasedimentary rock of Paleozoic age. MBT forms the boundary between Lower Himalaya and Sub Himalaya. Siwalik sandstone of folded and faulted the Tertiary sedimentary rock have been over thrusted in the south of MBT. Mahabharat Thrust (MT) separates crystalline rocks in the north from metasedimentary rock in the south. The general trend of Thrust is West-North-West to East-South- East and dips at 65° towards north east. The thrust crosses tunnel at chainage 1+450m chainage. MT can be considered as an extension of MCT. The Main MCT is formed due to collision of Indian plate during Cenezoic age. MCT appears to begin thrusting at 50 million years ago and continue today. The rate of northward movement is considered to be 5cm/year in recent years (NEA, 1997).

2. Seismicity of the Project Area

An analysis of 281 seismic events of earthquake records from 1913 AD to 1987 AD shows that the distribution of earthquake epicenter is due to MBT. All the earthquake epicenters near MBT were less than 5 in magnitude. The only location of earthquake with epicenter at distance 250 km west MBT have magnitude of 6.2. The estimated maximum peak horizontal acceleration related to MBT is 0.46g (NEA, 1997).

3. Site Investigation and Engineering Geology.

The geology of the project area consists of Redua Formation, Bhainsedobhan Marble, Kalitar Formation of Bhimpedi Group, Benighat Slate, Malekhu Limestone, Robang Formation of Upper Nuwakot Group and Siwalik Group overlain by Quaternary deposits of limestone breccias, terrace deposits, riverbed deposits and scree deposits. The area comprises of crystalline rocks as garnet-mica schist Marble, and meta sedimentary rocks as schists of Precambrian age and quartzite, phyllite, siliceous dolomite and slaty phyllite of Paleozoic age. Strike of formations is generally WNW-ESE. The boundary between Upper Nawakot Group and Bhimphedi Group is called the Mahabharat Thrust and Upper Nawakot Group and Siwalik Group are bounded by the Main Boundary Thrust (NEA,1997). A number of discontuinity or joint sets with distinctive and indistintive patterns have been observed along the tunnel alignment. The measured oreientation of tunnel axis and three distinctive joints sets obtained from NEA, 1997 have been stereographically projected in **Fig. 3**.

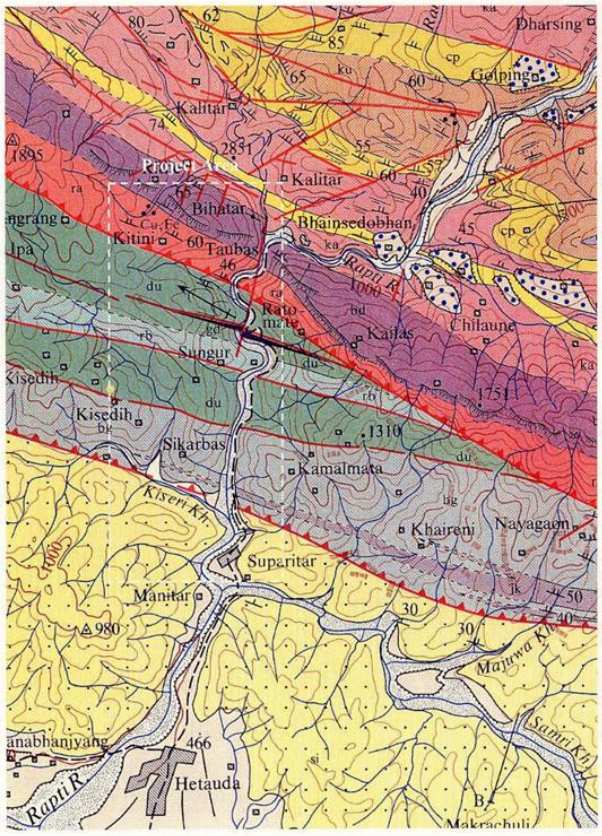

Fig. 1. Location of Kulekhani III Hydropower modified after NEA, 1997

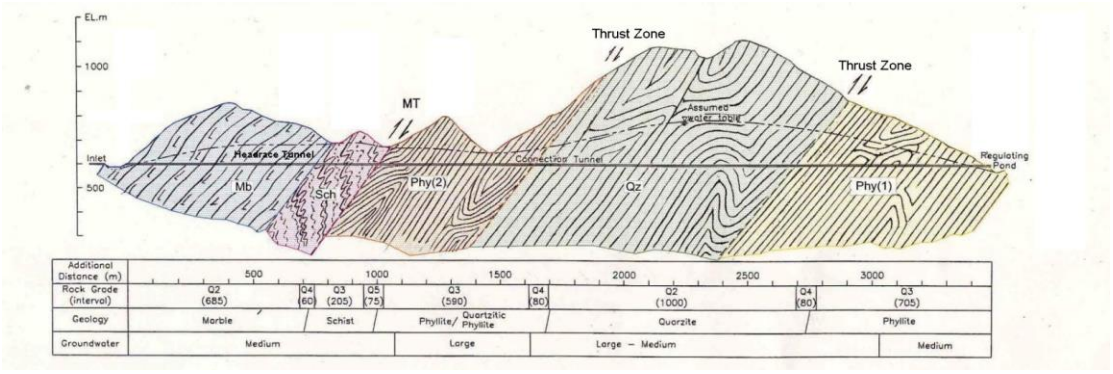

Fig. 2. Longitudinal section of Headrace tunnel of Kulekhani III Hydropower NEA, 1997.

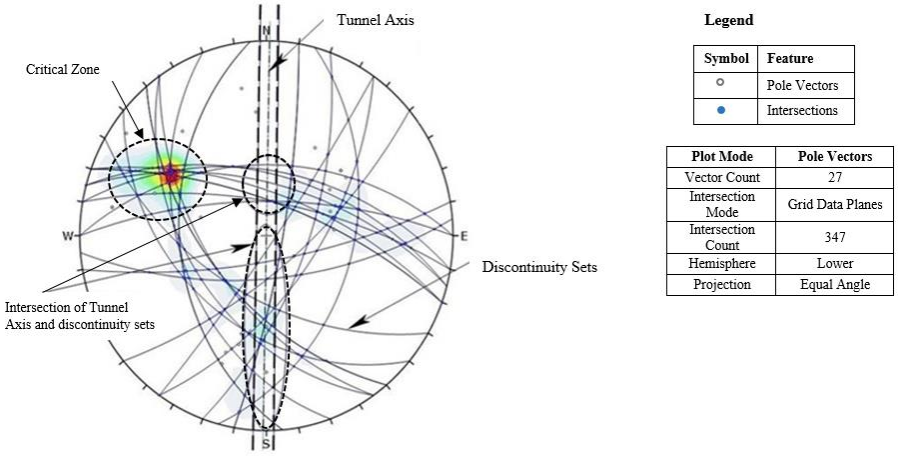

Fig. 3. Sterographic projection of discontuinity or joint sets along the headrace tunnel of Kulekhani III Hydroelectric Project.

Table 1. Rock mass classification according to Q system (NEA, 1997)

Chainage (m)		Rock Type	Q-value	Rock Mass Quality	Rock Support class
From	To				
0+000	0+170	Marble	6.25	Fair	R_2
0+170	0+715	Marble	10.6	Good	R_1
0+715	0+725	Sheared schist	0	Very Poor	R_4
0+725	0+990	Granetiferous schist	2.7	Poor	R_3
0+990	1+215	Quarzite schist	5	Fair	R_2
1+215	1+430	Schistose Quarzite	4.7	Fair	R_2
1+430	1+450	Sheared Schists	0	Very Poor	R_4
1+450	2+355	Quarzite	13.3	Good	R_1
2+355	3+635	Phyllite	2	Poor	R_3
3+635	3+650	Sheared Phyllite	0	Very Poor	R_4
3+650	3+965	Siliceous Dolomite	4.7	Fair	R_2
3+965	4+337	Slate Phyllite	2.3	Poor	R_3

The Strike and dip angle of 36 joint sets are presented in **Table 2** are projected in the steriograph. The strike of tunnel is 181°N. The stereograph is equal angle projection in lower hemisphere. The plot mode is vector mode with 27 number of vector counts.The intersection mode of grid data planes show that the majority of joint. planes intersect the tunnel axis in the perpendicular directions and with acute angle inclination. The intersection of the joint sets is more in the left of the tunnel axis (**Fig. 3**). The stereographic projection shows that all the joints intersect the tunnel alignment. Hence, it can be used in numerical modelling. (Satıcı and Ünver 2015).

4. Rock Support Estimation

In 2002, Barton et al. published the modified Q system of rock mass classification system to estimate the rock support by using schematic support chart.

$$Q=\frac{RQD}{J_n}\times\frac{J_r}{J_a}\times\frac{J_w}{SRF} \quad [1]$$

Where,
RQD=Rock Quality Designation,
J_n=Joint Set Number,
J_r=Joint Roughness Index,
J_a=Joint alteration number,
J_w=Joint Water Reduction Factor,
SRF=Stress Reduction Factor.

The value obtained from Eq. [1] gives a description of the rock mass quality. The different Q-values are related to different types of permanent support by means of a schematic support chart (Barton et al., 2002). This means that by calculating the Q-value it is possible to find the type and quantity of support that has been applied previously in rock masses of the similar qualities.

Therefore, the Q-system has been used as a guideline in rock support design decisions and for documentation of rock mass quality in Headrace tunnel of Kulekhani III Hydroelectric Project. The rock mass in headrace tunnel has been classified into 5 classes Q_1, Q_2, Q_3, Q_4 and Q_5. their corresponding support classes are R_1, R_2, R_3, R_4 and R_5 respectively. The values of Q for different classes are shown in Table 3. Similarly, the provided tunnel supports for different support class are shown in **Table 4**.

$$\sigma_1=\sigma_3+\sigma_{ci}\left(m\frac{\sigma_1}{\sigma_{ci}}+s\right)^{0.5} \quad [2]$$

Where,
σ_1=Maximum Principal stress,
σ_3=Minimum Principal stress,
σ_{ci}=Uniaxial Compressive strength,
m_b=Hoek Brown constant for the rock mass,
s=Constant depend upon the rock mass,
a=Constant depend upon the rock mass

$$m_b=m_i\exp\left(\frac{GSI-100}{28-14D}\right) \quad [3]$$

Table 2. Joint parameters modified after NEA, 1997

Rock Type	Joint Sets	Strike°	Dip°	Spacing(m)	Persistance(m)	Cj	ϕj°	Persistance in 1
Marble	J_1	020	70	2	15	0.05	20	0.5
	J_2	100	80	0.3	1	0.08	22	0.4
	J_3	265	40	0.5	1	0.08	22	0.75
Marble	J_1	020	70	2	15	0.06	22	0.4
	J_2	100	80	0.8	1	0.1	24	0.5
	J_3	265	40	0.5	1	0.09	24	0.5
Sheared schist	J_1	020	70	1	10	0.01	20	0.7
	J_2	100	80	0.8	1	0.02	20	0.5
	J_3	265	40	1	1	0.02	20	0.5
Granetiferous schist	J_1	360	50	0.5	10	0.01	18	0.7
	J_2	125	85	0.4	1	0.012	20	0.3
	J_3	230	55	0.3	1	0.012	20	0.2
Quarzite schist	J_1	010	50	0.5	0.8	0.1	25	0.4
	J_2	175	85	0.8	0.8	0.1	25	0.3
	J_3	230	55	0.5	15	0.07	20	0.8
Schistose Quarzite aDolomite	J_1	015	55	0.5	1	0.1	23	0.3
	J_2	110	65	0.4	15	0.08	20	0.8
	J_3	210	55	0.3	0.8	0.012	26	0.2
Sheared Schists	J_1	015	70	0.6	1	0.11	23	0.3
	J_2	110	55	0.5	10	0.1	22	0.6
	J_3	210	70	0.5	0.8	0.15	26	0.2
Quarzite	J_1	010	70	0.3	0.8	0.12	26	0.2
	J_2	235	55	0.6	15	0.1	22	0.9
	J_3	140	70	0.4	0.8	0.12	26	0.2
Phyllite	J_1	020	65	0.7	0.8	0.015	22	0.4
	J_2	235	45	0.5	0.8	0.015	22	0.3
	J_3	125	60	0.4	15	0.1	18	0.8
Sheared Phyllite	J_1	020	70	1	0.6	0.02	22	0.4
	J_2	235	40	0.6	0.5	0.02	22	0.3
	J_3	125	75	0.5	10	0.15	22	0.8
Siliceous Dolomite	J_1	360	70	0.6	1	0.015	22	0.4
	J_2	250	40	0.3	1	0.015	22	0.4
	J_3	170	75	0.4	15	0.1	20	0.8
Slate Phyllite	J_1	015	60	0.6	1	0.012	20	0.5
	J_2	105	40	0.6	0.5	0.012	20	0.4
	J_3	220	40	0.2	15	0.01	18	0.9

Table 3. Q value for different rock class (NEA,1997)

Rock class	Q value
Q_1	>40
Q_2	10 to 40
Q_3	4 to 10
Q_4	1 to 4
Q_5	<1

Table 4. Provided Rock supports for different support class (NEA, 1997)

Support class	Tunnel Supports
R_1	Untensioned cement mortar grouted rock bolts, Concrete lining(M25), Steel fibre reinforced shortcrete (5cm)
R_2	Untensioned cement mortar grouted rock bolts, Concrete lining(M25), Steel fibre reinforced shortcrete (5cm)
R_3	Untensioned cement mortar grouted rock bolts, Concrete lining(M25), Steel fibre reinforced shortcrete (5cm)
R_4	Untensioned cement mortar grouted Rock Bolts, Concrete lining(M25), Steel fibre reinforced shortcrete (10cm).
R_5	Untensioned cement mortar grouted rock bolts, Concrete lining(M25), Steel fibre reinforced shortcrete(10cm), Steel ribs ISMB 175.

5. Geotechnical Properties of Rockmass and Intact Rock

The geotechnical parameter of the intact rock and rock mass required for the numerical modelling were obtained from detailed design report of Kulekhani III Hydroelectric project by NEA,1997 .Seismic refraction survey(17 profiles of total length 1955 m), core drilling(3 holes of total length 105 m) , permeabilty test and core logging, test adits, discontuinity survey, rockmass classification, construction material survey, sampling and laboratory test such as point load test, water absorption test, rock shear Test were conducted to determine rock type support pressure, In-situ stress, strength parameters such as Uniaxial compressive strength, Intact rock mass modulus, poisson ratio, frictional angle, Unit weight, Peak and Residual Hoek Brown Residual strength parameters were obtained from laboratory tests(NEA, 1997).

The empirical relation given by Hoek et al., 2002 were used to obtain the peak rockmass properties (Eq. [2} to Eq. [7]). Similarly, GSI value of different rock type was obtained as suggested by Panthee et al.,2016. The geotechnical parameters and strength parameters for the discontuinities such as cohesion and internal friction angle, spacing, persistance were obtained as suggested by (Panthee et al, 2016; Özgür and Ünver, 2015) and presented in Table 1.

.

$$s=\exp\left(\frac{GSI-100}{28-14D}\right) \quad [4]$$

$$a=\frac{1}{2}+\frac{1}{6}\left(e^{-GSI/15}-e^{-20/3}\right) \quad [5]$$

$$\sigma_c=\sigma_{ci}s^a \quad [6]$$

$$\sigma_t=-\frac{s.\sigma_{ci}}{m} \quad [7]$$

Where,
σ_c=Compressive Strength of Rock mass,
σt =Tensile Strength of Rock mass

The rock mass properties around the tunnel perimeter will not remain same as excavation progresses. It will get disturbed (Cai et al., 2007) due to excavation method such as drilling and blasting Heading and benching which was used during the excavation of the Kulekhani III Headrace Tunnel. So to establish the realistic model with the effect of the excavations, the residual Hoek Brown strength parameters such as m_i, m_b, s, and GSI are calculated using the empirical relation given by (Cai et al., 2007: Hoek and Diederichs, 2006). Similarly, modulus of elasticity and GSI of residual rock mass were obtained as suggested by Hoek and Diederichs, 2006 and Cai et al., 2007 (Eq. [8] and Eq. [9])

$$E_{rm}=E_i\left(0.02+\frac{1-D/2}{1+e^{(60+15D-GSI)/11}}\right) \quad [8]$$

$$GSI_r=GSI.e^{-0.134\times GSI} \quad [9]$$

Where,
E_{rm}=Modulus of Elasticity of Rock mass,
E_i=Modulus of Elasticity of Intact Rock

The internal angle and cohesion was calculated by using the relation of equivalent Mohr Column parameters given by Hoek and Brown in 2002. (Eq. [10] and Eq. [11])

$$\phi = \sin^{-1}\left[\frac{6am_b(s+m_b\sigma_3)^{a-1}}{2(1+a)(2+a)(s+m_b\sigma_3)^{a-1}}\right] \quad [10]$$

$$c=\sigma_{ci}\left[\frac{[(1+2a)s+(1-a)](s+m_b\sigma_3)^{a-1}}{(1+a)(2+a)\sqrt{6am_b(s+m_b\sigma_3)^{a-1}/(1+a)(1-a)}}\right] \quad [11]$$

Where,
c=Cohesion of rockmass,
ϕ=Friction angle of rockmass.

$$\sigma_1 = Y.H \quad [12]$$

$$\sigma_3 = \frac{U}{1-U}Y.H+\sigma_{tectonic} \quad [13]$$

For the calculation of field stress in faulted rock mass the vertical stress generated due to gravitational loading is calculated from Eq. [12] and horizontal stress given by Jaeger and Cook in 1971 is calculated from Eq. [14].

According to Shrestha and Panthi, Eq. [13] gives the relation of the principal stresses σ_1 and σ_3 in the faulted rock mass in Nepal Himalaya. The back calculation done by Shrestha and Panthi in faulted Modi Khola Pressure Tunnel calculates the principal stresses σ_1=2.08MPa and σ_3=1.33MPa which is similar to the values σ_1=2.08MPa and σ_3=1.39MPa given by Eq. [14] by Jaeger and Cook in 1971. The equation is obtained from 2D Faulting theory which assumes that the failure is only a function of the difference between the principal stresses σ_1 and σ_3 (Zoback and Zoback, 2002). Hence, it can be suggested that the equation given by Jaeger and Cook in 1971 (Zoback and Zoback, 2002) can be used to empirically estimate the principal stresses in Faulted Rock Mass in Nepal Himalaya.

$$\frac{\sigma_1}{\sigma_3} = \left(\left(U^2+1\right)^{\frac{1}{2}}+U\right)^2 \quad [14]$$

6. Numerical Modelling

During the excavation of the tunnel, there will always be the time gap between the excavation, hauling and tunnel supports. The rock mass around the tunnel loose its stiffness during this period (Kavvadas, 2005) and geotechnical parameters lessen to their residual values depending upon the magnitude, direction of the in-situ stresses and post failure behavior of the rockmass (Cai, 2007; Kwon et al., 2009).

The inverted D-shaped tunnel of diameter 3.5 m with the external boundary 6 times the diameter of the tunnel has been modelled. The model has been fixed from top, bottom and both sides. Mesh and discretization was generated automatically by the software and three noded traingles were chosen as mesh element. The geotechnical parameters of the rock mass have been used as calculated in **Table 5**. The joints parameters have been incorporated in the model using the measured orientation and calculated strength parameters in Table 1.

The behavior of the rock mass after yielding can only be simulated with the plastic deformations (Cai et al, 2007). Hence, the plastic analysis has been done.

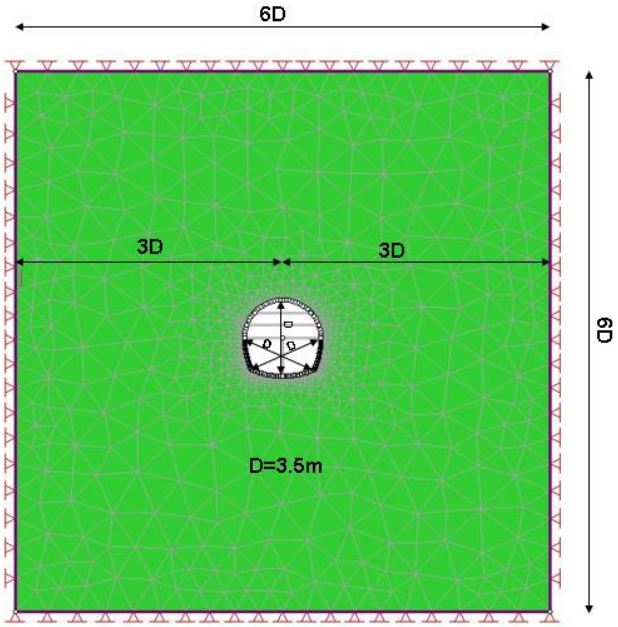

Fig. 4. Tunnel without joints

The heading and benching method can be used to demonstrate the time gap between excavation, hauling and supporting in the model. But it is very difficult to obtain the relaxation stage in the jointed rock mass for the support installation. It is because of the fact that the jointed rock mass is very weak and yielding is inevitable to occur in the boundary of each joint. In this case, the load split method suggested by (Khadka et al., 2016) is used. The load split method has been used for the simulation of the relaxation of the tunnel for the installation of the tunnel supports. The load split factor of 0.7 has been used in first stage after the excavation and support is installed and load factor of 0.3 has been used in the second stage (Khadka et al., 2016).

The main aim of the study is to study the effect of the faults and joints and to determine tunnel supports in faulted rock mass with the discontinuities in Nepal Himalaya. So, two models with the same modelling conditions and parameters are made in RS2., First model was incorporated with the joint parameters as shown in **Fig. 4** and second model was without the joint parameters in **Fig. 5**. Hoek and Brown Failure criteria was chosen as failure criteria because the rock mass is controlled tightly by interlocking angular rock masses and joints. The original Hoek Brown failure criteria was found to work well with this kind of the rock masses (Hoek et al, 2002).

In massive case, continuum modelling approach was represented (Hammah et al.,, 2008) and discontuinity sets added model represents discontinum modelling (C. Torres et al., 2000). The model without the joints is a continuum model in which the stress and the deformation behavior is isotropic. Whereas in the discontinuum model with the joints, distribution of the stress and deformation is anisotropic in nature. Due to which there is degradation of the strength parameters of the rock mass (Su et al., 2017). Therefore, a realistic numerical model should be modelled to incorporate the phenomenon. (Vlachopoulos and Diederichs, 2009).

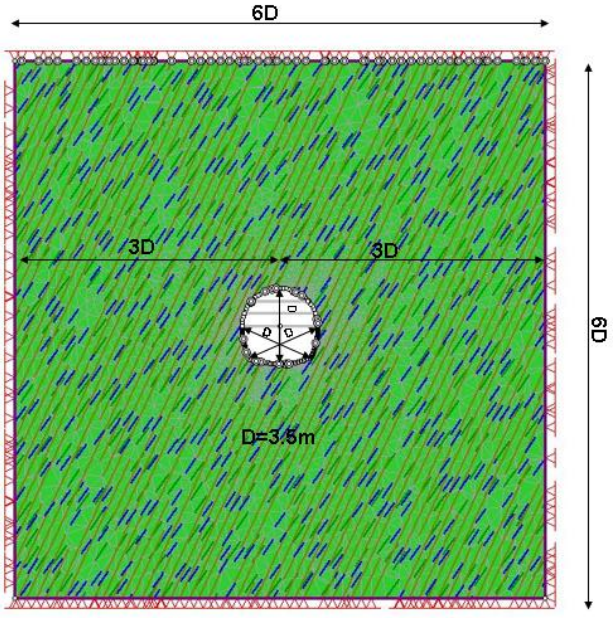

Fig.5. Tunnel with joints

Plane strain Model with the joints have been generated using Phase2. Discrete fracture networks (DFN) of the joints have been created using automatic joint network generator. The parallel deterministic joint model has been used with closed ends. The orientations, spacings, persistence, cohesion, frictional angle of the joints at different chainage are given in **Table 2**.

The analysis of the models shows that there was more failed or yielded rock mass in the jointed model in comparsion to the model without the joints. At Chainage 0+715 m to 0+725 m, in unjointed model the total no of yielded elements was 517with the total displacement of 12.6mm whereas in jointed model the total no of yielded elements was 666 with total displacement of 14.8 mm. At Chainage 1+430 m to 1+450 m, in unjointed model the total no of yielded elements was 569 with the total displacement of 7.4 mm whereas in jointed model the total no of yielded elements was 1340 with total displacement of 36.6 mm. Similarly, At Chainage 3+635 m to 3+650 m, in unjointed model the total no of yielded elements was 2084 with the total displacement of 20.13 mm whereas in jointed model the total no of yielded elements was 2573 with total displacement of 45.6 mm. The yielded elements at different chainage is illustrated in the **Fig.6**. It can clearly be seen that the no of yielded elements is more in jointed rock mass in comparison to that of unjointed rock mass.

The support was then installed to prevent the failure or yielding of the rock mass. The provided supports included bolts of diameter 25 mm at spacing of 2 m, Fibre reinforced shortcrete of 5 cm and Concrete lining of 25 MPa, Steel ribs ISMB 175 (**Fig. 9**) The number of the yielded elements and the displacement decreased. But support capacity curvre showed that the support was not sufficient. The support failed to resist the thrust and moments. The support failed in the crown, invert and side walls. So, the thickness of the reinforced concrete was increased to 0.4 m. Then the analysis was run again but the support capacity curve showed that the support was still insufficient. So the support was increased to 0.6m, 0.8 m and 1 m respectively.

The modelling results showed that total thickness of the support (concrete lining and fibre reinforced shorcrete) of greater than 1m was required to resist the in-situ stress and loading in the discontinous rock mass. But this support is practically not feasible as it would change the dimensions of the tunnel and it is very difficult to install the support in tunneling. Therefore, for the safe and feasible support, two measures have been adopted. The first measure is forepoling. Forepoling is used to reinforce the rock mass around the tunnel as proposed by Evert Hoek in an unpublished notes . The second measure is changing the rock mass properties around the tunnel. In 2001, Hoek proposed that weak rock mass near the tunnel gets disturbed more than at the farther distance from the tunnel.

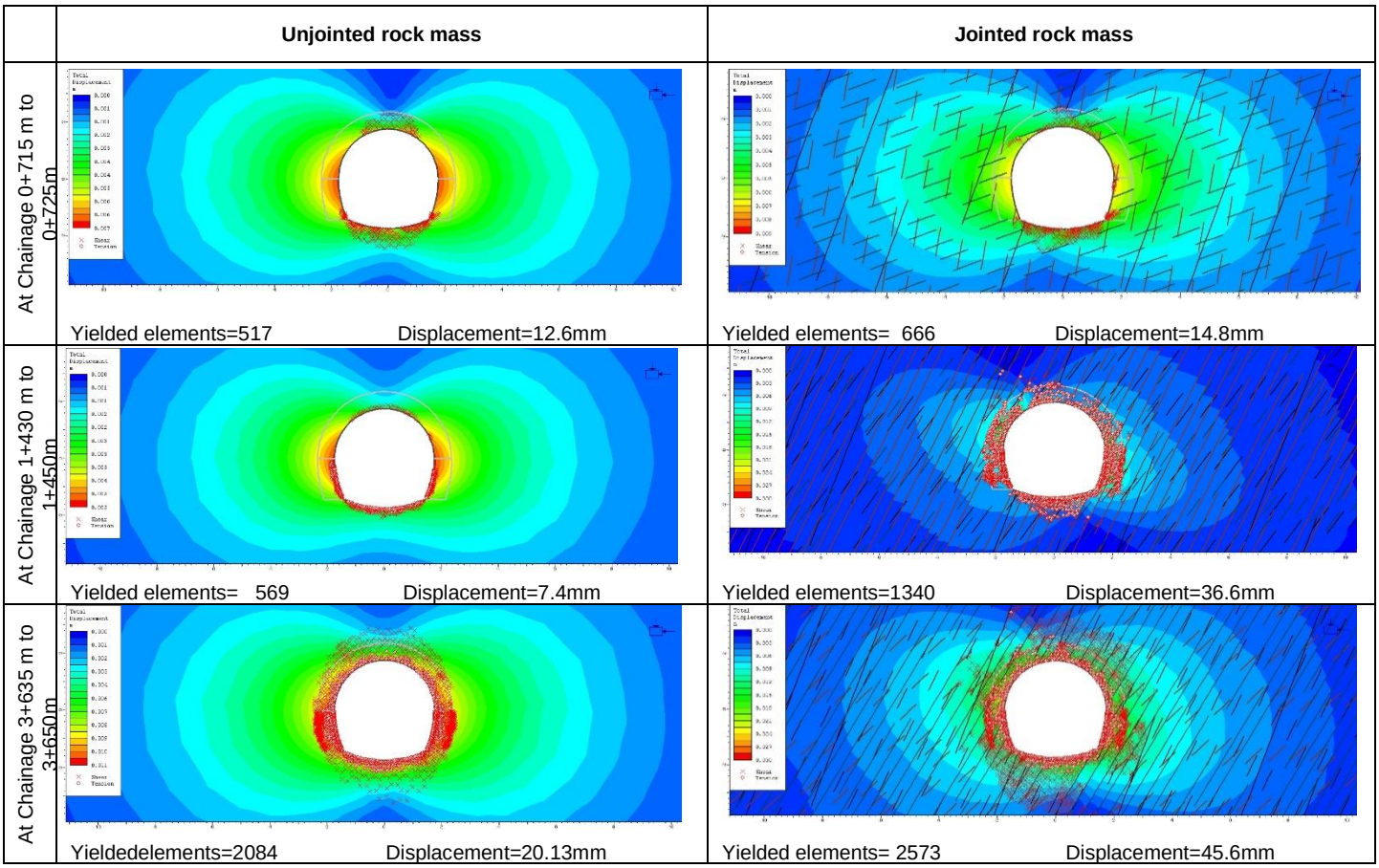

Fig. 6. Yielded elements and displacement at different chainage

This decreases the strength parameters of the rock mass around the tunnel boundry more in comparision to that of rockmass at farther from the tunnel. The rock mass properties with the Disturbance factor 0.5 have been used up to the distance of 1.5 D from the center of the tunnel and Disturbance factor of 0 have been used for the rock mass between the distance of 1.5 D to 3 D (**Fig. 7** & **Fig. 8**).

Forepoles having external diameter of 114 mm and internal diameter of 100 mm spaced at 0.5 m have been used to reinforce the rock mass around the tunnel. To model the effect of the forepoles, the equivalent rock mass properties are estimated from the Hoek Brown Failure Criteria. The equivalent rock parameters are then modelled with thickness of 0.6 m (**Fig. 7** & **Fig. 8**). Also the properties of the rock mass around the tunnel have been modified as suggested by Hoek in 2001. The modulus of the elasticity of the rock mass is calculated with D=0 and D=0.5 from Eq. [8].

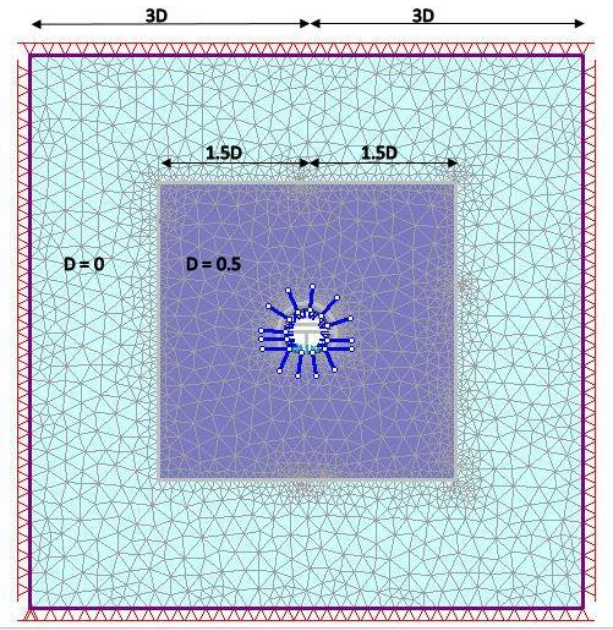

Fig. 7. Model with forepoling and different rock mass properties without joints

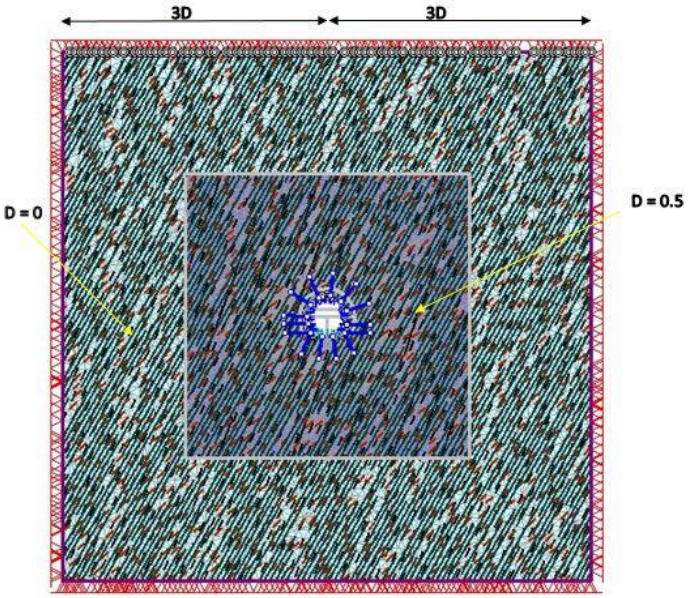

Fig. 8. Model with forepoling and different rock mass properties with joints

The model was then analysed again with the reinforced concrete of 0.2m, rock bolts of 25mm diameter, 3 Bar lattice girder. But the added support was still not sufficient, as the support capacity curve showed that the support at the base of the wall, crown and invert failed. The thickness of the concrete and grade of the concrete was increased gradually and the respective support capacity curve was plotted.

The support capacity curve showed that the support installed was still failing to resist the loads. The failure was concentrated in the crown and bottom of the side walls.

The support combination of reinforcement of the concrete with the rebar of diameter 43 mm with the effective depth of 250 mm, three bar lattice girder (50, bar size 18, 26 mm), concrete of thickness 400 mm of 45Mpa, and bolts of diameter 35 mm of length 3 m at spacing 1 m was used (**Fig. 10**). The support capacity curve of this combination showed that the support was safe (**Fig. 11**).

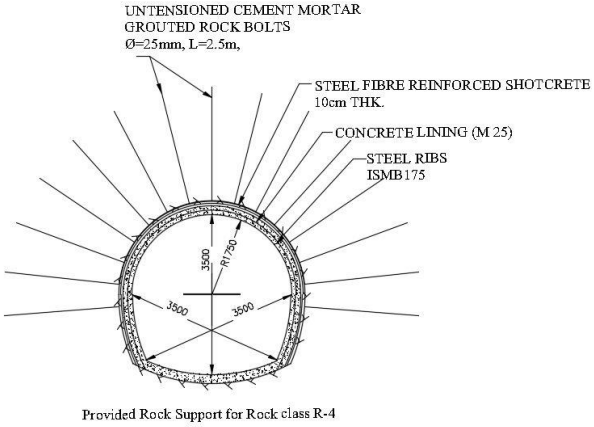

Fig. 9. Provided Rock Supports for R-4 (NEA 1997)

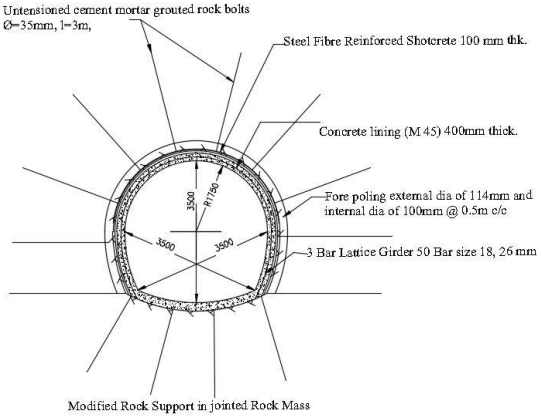

Fig. 10. Modified Rock Supports for R-4

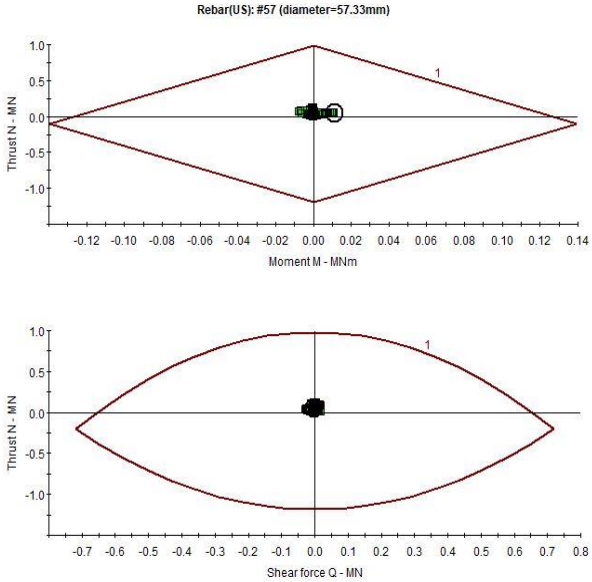

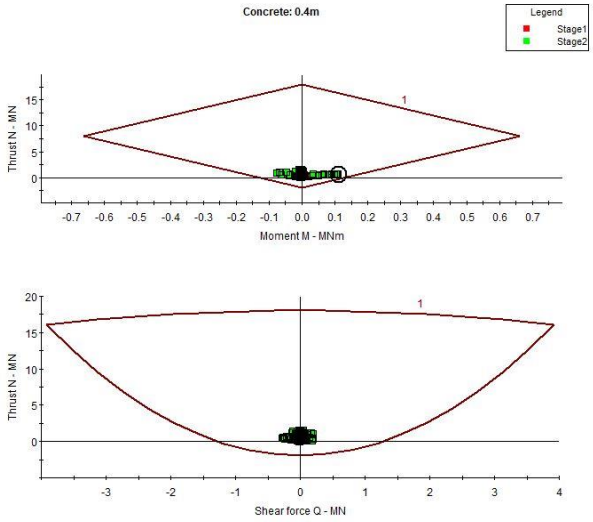

Fig. 11. Support capacity curve (RS2)

7. Conclusion

The equal angle stereographic projection in the lower hemisphere of joint sets and tunnel axis helps to determine their relative angle of the joint sets and tunnel axis. The joint sets with acute angle with the tunnel axis is incorporated in the 2 D numerical modelling in RS2. The empirical equation given by Jaeger and Cook in 1971 (Eq. [14]) can be used to determine the principal in-situ stress in the faulted rock mass in Nepal Himalaya. The calculated principal stresses due to the fault is used to simulate its effect in 2 D numerical model.

In the case of faulted and jointed rock mass, load split method for the support installation is used for the numerical modelling. Hoek Brown failure criteria is used for the analysis for jointed and faulted rock mass. The comparative numerical modelling suggested that the rock mass with the fault and joints is very weak with high deformation and yielding in comparison to rock mass without fault and joints. The estimated support using rock mass classification (Q-system) have proved to be inadequate. Therefore, to provide safe and feasible support, two measures have been used to reinforce and strengthen the rock mass around the tunnel. The two measures are Forepoling and Changing the rock mass properties. These two measures help to reduce the deformation and yielding of the rock mass around the tunnel. Hence, we can conclude that the tunnel support required for the faulted rock mass and jointed rock mass can be estimated by using the numerical analysis in RS2 commercial software by Rocscience.

Acknowledgements

The authors would like to express their sincere gratitude for financial supports from the University Grant Commission and Faculty Research Grant under grant UGC/FRG-73/74-ENGG-03 and also to Kulekhani III Hydroelectric project team for providing us the necessary data and materials for study.

References

Anagnostou, G. and Kovári, K., 2005, Tunnelling through geological fault zones. Proceedings of International symposium on design, construction and operation of long tunnels. Taipei, Taiwan: ETH-Zürich..

Barton, N. ,2002, Some new Q-value correlations to assist in site characterisation and tunnel design, International Journal of Rock Mechanics & Mining Sciences 39, 185–216.

Cai, M., Kaiser, P. K., Tasaka, Y., And Minami M.,2007, Determination of residual strength parameters of jointed rock masses using the GSI system. International Journal of Rock Mechanics and Mining Sciences, Volume 44, Issue 2, 247-265. .

Hammah, R. E., Yacoub, T., Corkum, B., and Curran, J. H., 2008, The Practical Modelling of Discontinuous Rock Masses with Finite Element Analysis, American Rock Mechanics Association

Hoek, E. and Diederichs, M.S., 2006, Empirical estimation of rock mass modulus, International Journal of Rock Mechanics & Mining Sciences 43, 203-215.

Hoek, E., Torres C.C., Corkum B.,2002, The Hoek–Brown Failure Criterion- 2002 edition.

Hoek, E.,2001, Big Tunnels in Bad Rock, Journal of Geotechnical and Geoenvironmental Engineering 127(9).

Hoek, E., and Brown, E.T., 1997, Numerical Modelling for Shallow Tunnels in Weak Rock(Unpublished).

Kang, Y., Liu, Q., Xi, H., and Gong, G., 2018, Improved compound support system for coal mine tunnels in densely faulted zones. Engineering Geology, Volume 240, 10-20.

Kavvadas, M. ,2005, Monitoring ground deformation in tunnelling: Current practice in transportation tunnels, Engineering Geology 79(1), 93-113.

Khadka, S. S.,2019, Tunnel closure analysis of hydropower tunnels in lesser himalayan region of nepal through case studies, Dhulikhel, Kavre, School of Engineering, Kathmandu Univeristy. DOI:10.13140/RG.2.2.35884.41607http://rmlab.ku.edu.np/publications.

Khadka, S. S., Gomes, A., M., T., Jeon, S., and Maskey, R., M., 2016, Comparative numerical study of 2d and 3d finite element modeling of hydropower tunnel: case study from lesser himalayan region of Nepal,Conference: 15CNG_8CLGB. Porto, Portugal , University of Porto. http://rmlab.ku.edu.np/publications.

Kwon, S., Lee, C., Cho, S. J., and Jeon, S., 2009, An investigation of the excavation damaged zone at the KAERI underground research tunnel. Tunnelling and Underground Space Technology 24(1), 1-13.

Mezzatesta, F., Malaguti, A.,2010, Yielding Support Design In Ceneri Base Tunnel, ISRM International Symposium - EUROCK 2010, 359-362.

Nepal Electricity Authority (1997). Detailed Design Report of Kulekhani III Hydroelectric Project. Kathmandu, Nepal.: Nepal Electricity Authority.

Özgür, S. And Bahtiyar Ü.,2015, Assessment of tunnel portal stability at jointed rock mass: A comparative case study,Computers and Geotechnics 64, 72-82.

Panthee, S., Singh, P., K., Kainthola, A., and Singh, T., N., 2016, Control of rock joint parameters on deformation of tunnel opening. Journal of Rock Mechanics and Geotechnical Engineering, Volume 8, Issue 4, 489-498.

Russo M., Germani G., and Amberg W., 2002, Design and construction of large tunnel through active faults: a recent application, International Conference of Tunnelling & Underground Space Use. Istanbul, Turkey.

Shrestha, P. K., And Panthi, K. K., 2014, Groundwater Effect on Faulted Rock Mass: An Evaluation of Modi Khola Pressure Tunnel in the Nepal Himalaya,Rock Mechanics and Rock Engineering,Volume 47, Issue 3, 1021–1035

Sunuwar, S. C.,2005, Problem of shear zones and faults in construction of infrastructures in the Nepal Himalaya, Fifth Asian Regional Conference on Engineering Geology for Major Infrastructure Development and Natural Hazards Mitigation, Kathmandu, Nepal: Journal of Nepal Geological Society.

Su, H., Jing, H., Yu, L., and Wang, Y.,2017, Strength degradation and anchoring behavior of rock mass, Environmental Earth Sciences 76(4), 179.

Torres, C.C. and Fairhurst. C., 2000, Application of the Convergence-Confinement Method of Tunnel Design to Rock Masses that Satisfy The Hoek-Brown Failure Criterion, Tunnelling and Underground Space Technology 15(2), 187-213.

Vlachopoulos, N., amd Diederichs, M., S., 2009 Improved longitudinal displacement profiles for convergence confinement analysis of deep tunnels, Rock Mechanics and Rock Engineering, 42(2), 131–46.

Zingg, S., and Anagnostouv, G., 2012, Tunnel Face Stability In Narrow Water-bearing Fault Zones, ISRM International Symposium - EUROCK 2012, Stockholm, Sweden: International Society for Rock Mechanics and Rock Engineering.

Zoback, M. D., And Zoback, M. L., 2002, Chapter 34 State of stress in Earth's Lithosphere, International handbook of Earthquake and Engineering Seismology, part 1 (p. 1200). Elsevier

Symbols and abbreviations

MBT	Main Boundary Thrust.
MFT	Main Frontal Thrust
MCT	Main Central Thrust
MT	Mahabharat Thrust
C_J	Cohesion of joints
ϕ_J	Friction angle of joints
RQD	Rock Quality Designation
J_n	Joint Set Number
J_r	Joint Roughness Index
J_a	Joint alteration number
J_w	Joint Water Reduction Factor
SRF	Stress Reduction Factor
σ_1	Maximum Principal stress
σ_3	Minimum Principal stress
σci	Uniaxial Compressive strength
m_b	Hoek Brown constant for the rock mass
s	Constant depend upon the rock mass
a	Constant depend upon the rock mass
GSI	Geological Strength Index
D	Disturbance factor
σc	Compressive Strength of Rock mass
σt	Tensile Strength of Rock mass
E_{rm}	Modulus of Elasticity of Rock mass
E_i	Modulus of Elasticity of Intact Rock
GSI_r	Residual Geological Strength Index
γ	Unit weight of Rock mass
H	Overburden